Detection of nitroaromatic vapours with diketopyrrolopyrrole thin films: exploring the role of structural order and morphology on thin film properties and fluorescence quenching efficiency

Article

Accepted Version

Journal Name

Dynamic Article Links ►

Cite this: DOI: 10.1039/c0xx00000x

www.rsc.org/xxxxxx

ARTICLE TYPE

Detection of nitroaromatic vapours with diketopyrrolopyrrole thin films: Exploring the role of structural order and morphology on thin film properties and fluorescence quenching efficiency

Monika Warzecha,[a] Jesus Calvo-Castro,[a] Alan R. Kennedy,[b] Alisdair Macpherson,[c] Kenneth Shankland,[d] Norman Shankland,[e] Andrew J. McLean[a*] and Callum J. McHugh[a*]

Received (in XXX, XXX) Xth XXXXXXXXX 20XX, Accepted Xth XXXXXXXXX 20XX

DOI: 10.1039/b000000x

Sensitive optical detection of nitroaromatic vapours with diketopyrrolopyrrole thin films is reported for the first time. The impact of thin film crystal structure and morphology on fluorescence quenching behaviour is demonstrated, such that by judicious control over film fabrication, highly effective detection of important nitroaromatic targets is realised.

Novel approaches to detection and identification of explosives is a field of significant worldwide importance.[1,2] To combat modern day global uncertainties, detection systems should be simple, inexpensive, robust and able to quickly identify a diversity of species.[3] Significant progress has been made in optical based methods and recent reviews highlight that this area shows great promise for future developments.[4,5] To date the most successful strategies are based upon solid state fluorescent materials and modulation of analyte response via electron transfer. Ubiquitous in this field are conjugated polymers based upon poly-(phenylene-ethyylene) and poly-(phenylene-vinylene) derivatives, developed by the Swager group.[5,6] Pentiptycene and dibenzochrysene derivatives commercialised in the Fido® XT system are selective and sensitive, with vapour response to nitroaromatic explosives in the femtogram range.[7] Other notable examples include polysilanes and polymetalloles,[8] small molecule microarrays,[9] fluorescent porous silica,[10] nanowire arrays,[11] nanofibril films,[12] molecularly imprinted polymers,[13] calix[4]arenes[14] and metal organic frameworks.[15] Despite significant advances, improvements in sensor cost, adaptability, portability, size and complexity would be major innovations that could be realised via development of new optical and electronic based technologies.[16,17]

In this regard, we are engaged in development of diketopyrrolopyrrole (DPP) small molecule semiconductors and recently reported high computed charge transfer integrals in DPP motifs displaying cofacial π-stacking in the solid state.[18] These derivatives and structural analogues also exhibit efficient solid state emission and display high light and thermal fastness. Thus, they make promising candidates as signal transducers in *both* optical and electronic sensing environments. We report herein, for the first time, the *optical* behaviour of two DPP architectures whose solutions and thin films undergo effective fluorescence quenching upon exposure to nitroaromatics such as 2,4,6-trinitrotoluene (TNT), 2,4-dinitrotoluene (DNT) and nitrobenzene (NB). Crucially, the solid state vapour response towards these important targets is shown to be strongly influenced by the solid state structure and morphology of the DPP thin film environment.

Seventeen symmetric and asymmetric DPP derivatives containing groups designed to interact with electron deficient nitroaromatics, including alkoxy, amine and halogen functionality were prepared, isolated and characterised. The DPPs were assessed on their ease of synthesis, stability, film forming behaviour and electronic properties, including solution and solid state fluorescence response to NB, DNT and TNT. We report the optimal DPP structures as the hydro-benzyl and butoxyphenyl-benzyl derivatives **HBDPP** and **BBDPP** respectively (Scheme 1).

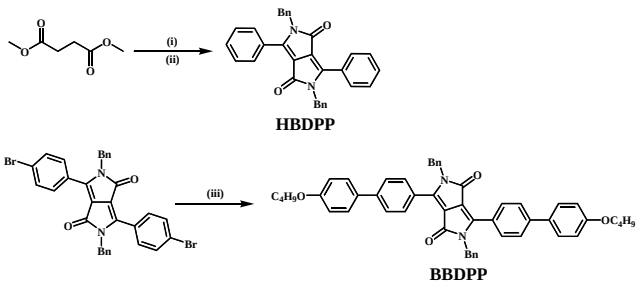

Scheme 1 (i) PhCN, Na, t-amyl alcohol, 120 °C; (ii) BnBr, K_2CO_3, DMF, 120 °C; (iii) $Pd(OAc)_2$, SPhos, 4-butoxyphenylboronic acid, K_3PO_4, THF

As reported by us previously, the single crystal structure of **HBDPP** is dominated by a long molecular axis, slipped (4.50 Å) cofacial π-π stacking arrangement along the crystallographic *a*-axis, with an intermolecular separation of 3.44 Å.[18] A single crystal structure of **BBDPP** was herein obtained to rationalise packing effects on its thin film properties and quenching performance (SI.2). The structure of **BBDPP** is consistent with **HBDPP** with a slipped cofacial stacking arrangement (despite the size and conformational flexibility of the butoxyphenyl substituents). In **BBDPP** however, the phenyl torsion is increased to 29 ° (c.f. 20 ° in **HBDPP**) and the long axis slip in the centrosymmetric monomer pairs reduced to 3.45 Å along the crystallographic *b* axis, with a further reduction in intermolecular separation to 3.37 Å. Accordingly, we propose given the presence of the cofacial intermolecular interactions that optical behaviour of both single crystals should be consistent with H-aggregates.[19]

Optical and electrochemical data in dichloromethane solution and from bulk material in the solid state are collated in (SI.3). In short, solution absorption spectra for both DPPs were broad with no vibronic structure; the bathochromic shift of λ_{max} in **BBDPP** attributed to phenyl versus H substitution. Fluorescence emission spectra in solution for each were also similar, with resolved vibronic structure observed. Solution fluorescence quantum yields ϕ_F, were high for **HBDPP** and **BBDPP** (0.85 and 0.81 respectively) and insensitive to oxygen quenching, greatly enhancing their potential application in working environments. Kubelka-Munk derived absorption spectra of both powders were broad and hypsochromically shifted compared to solution; a reduction in the absorption maximum in the solid state compared with solution (439 nm vs. 464 nm and 471 nm vs. 492 nm for **HBDPP** and **BBDPP** respectively) consistent with the blue shift expected from cofacial H-aggregates. Solid state fluorescence emission spectra of **HBDPP** and **BBDPP** were red shifted compared to solution (612 nm and 635 nm respectively), however from thin film data (vide infra) the large Stoke's shift in the powders is consistent with self-absorption effects.

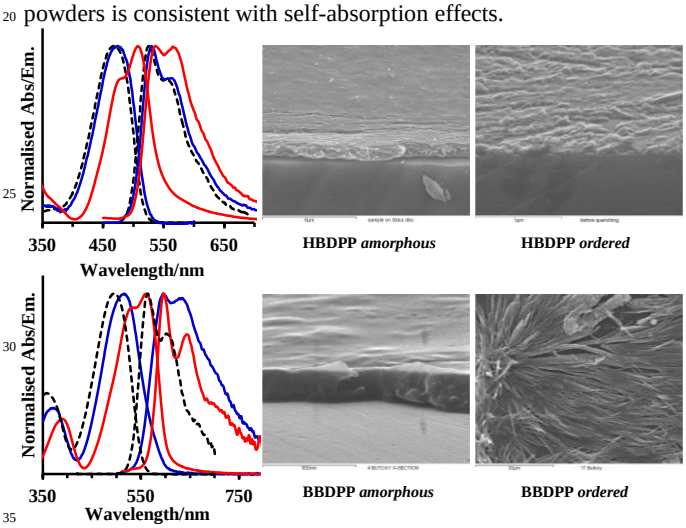

Fig. 1 **HBDPP** (top) and **BBDPP** (bottom) absorption and emission spectra from solution (black dash), amorphous (blue) and *as-deposited* ordered thin films (red). SEM images of amorphous and *as-deposited* ordered **HBDPP** and **BBDPP** films

Steady state fluorescence emission from **HBDPP** and **BBDPP** in dichloromethane solution was quenched upon exposure to NB, DNT and TNT under aerated conditions (SI.4). From fluorescence lifetimes (6.46 ns for **HBDPP** and 3.95 ns for **BBDPP**) and extracted K_{SV} data derived via Stern-Volmer analysis the quenching rate constants (3.84×10^9, 7.67×10^9 and 1.25×10^{10} $M^{-1}s^{-1}$ for **HBDPP** and 3.33×10^9, 9.50×10^9 and 1.16×10^{10} $M^{-1}s^{-1}$ for **BBDPP** with NB, DNT and TNT respectively) were determined and found to approach the calculated diffusion controlled rate limit (SI.4); the increase in k_q consistent with an increase in reduction potential of the quencher. Linearity in the Stern-Volmer plots at high quencher concentration accompanied by no change in the DPP absorption spectra was consistent with a dynamic quenching process. In addition, oxidation and reduction potentials of **HBDPP**, **BBDPP** and the nitroaromatics were determined by cyclic voltammetry; calculation of ΔG using Equation S4.2. (-0.103, -0.317 and -0.562 eV for **HBDPP** and -0.070, -0.285 and -0.530 eV for **BBDPP** with NB, DNT and TNT respectively) and comparison of HOMO and LUMO energies derived via the electrochemical analysis clearly demonstrating that in solution, electron transfer was thermodynamically favourable in both cases (SI.4).

Fluorescent thin films of **HBDPP** and **BBDPP** displaying varying thickness, structure and morphology were prepared on SiO_2 by spin coating from dichloromethane. Film thickness determined by surface profiling was shown to correlate well to absorbance (SI.5). Amorphous films of **HBDPP** and **BBDPP** were prepared from filtered dye solutions, and characterised by SEM and absorption and emission spectra, which for **HBDPP** were almost identical to those observed in solution (Fig. 1). Structured **HBDPP** films exhibiting higher long range order were obtained via seeding during spin coating; SEM analysis of the *as-deposited* films showing nanocrystalline islands of the dye (Fig. 1). Enhanced order in these films was supported by absorption and emission spectra which were red shifted compared to the amorphous films and which exhibited vibronic structure and a smaller Stokes shift; an increase in the intensity of the 0-1 transition in the absorption and emission spectra with respect to the 0-0 band indicating the presence of an H-aggregate and a structure consistent with that observed in the single crystal (Fig. 1).[19] In contrast, ordered **BBDPP** films displayed a fibrous morphology and a red shift in their absorption spectra with the emergence of vibrational structure at 535 nm and 561 nm. Contrary to structured **HBDPP** films, there was no red shift in the emission spectra with well resolved bands observed at 597 nm and 643 nm (Fig. 1). Amorphous **BBDPP** films were characterised by instability, with conversion of their absorption and emission spectra to those of ordered films upon thermal or solvent annealing; consistent with transformation of a kinetically trapped structure in the initially deposited film, to a more stable form. We have recently reported that N-benzyl DPPs can adopt various slipped cofacial orientations over their long molecular axis.[18] Chloro-substituted N-benzyl DPP polymorphs display either H or J-aggregate stacking interactions with either structure a minimum on the computed dimer potential energy surface (with the cofacial H-aggregate closest to the global energy minimum). In amorphous films of **BBDPP**, conversion to the more stable film affords a red shift and emergence of vibronic structure in the absorption spectra (where the 0-0 band is more intense than the 0-1) and a greater relative intensity of the 0-0 to 0-1 band in the emission spectra (Fig. 1). Both effects in progression from amorphous to ordered films are consistent with J-aggregation and slipped cofacial structure.[19] Thus, the H-aggregate **BBDPP** in the single crystal may not be the most stable thin film form and the greater stability of the ordered *as-deposited* films, and their associated fibrous morphology, is consistent with a slipped long molecular axis J-aggregate (vide infra).

Quenching of thin film emission was investigated using a modified version of the method reported by Swager (SI.5).[5,6] Exposure of amorphous films of **HBDPP** to either NB or DNT (a headspace marker for TNT)[20] vapour gave complete reduction of fluorescence intensity with the time taken to reach maximum quenching dictated by film thickness, accessibility of largely monomeric emissive sites in these films and the quencher vapour pressure (Fig. 2a&b). Accordingly, rapid and complete quenching

(a)

from 100 nm thick amorphous films of **HBDPP** fluorescence by NB was achieved after only 9 minutes, highlighting the efficient quenching in these films (Fig. 2a). For DNT, the dependence of film thickness on quenching rate was similarly observed, although in this case the overall quenching process was slower and consistent with the lower vapour pressure of DNT,[6] resulting in only 60 % of the total **HBDPP** emission being quenched after 480 minutes for a 180 nm thick film (100 % quenching being observed after overnight exposure to DNT). For amorphous **BBDPP** films a similar relationship was observed between NB and DNT quenching; NB producing a more rapid reduction in emission. However, for these films the time taken to reach quenching saturation was longer than for **HBDPP** films and the relationship between film thickness and quenching rate was reversed (SI.5). Exposure of amorphous **BBDPP** films to NB or DNT vapour also produced large changes to their absorption and emission spectra, associated with a change in film structure to the proposed J-aggregate conformation (SI.5). Thus, amorphous **BBDPP** films were not considered to be suitable as stable nitroaromatic sensing platforms as reduction in fluorescence emission could not be attributed purely to a quencher-fluorophore interaction. In contrast, ordered **BBDPP** films were stable to both NB and DNT vapours with no change in their absorption or emission spectra (SI.5). Exposure to NB and DNT gave rapid reduction of film fluorescence with comparable performance to that reported previously in other systems[4,5,15,21,22] (Fig. 2d). For 100 nm thick films, over 30 % of the total emission intensity was quenched within 2 minutes of exposure to NB vapour. With DNT, a greater degree of overall quenching was observed (45 % at saturation) although the quenching rate was lower compared to NB (15 % quenched after 2 minutes); the former due to the increased reduction potential and improved electrostatic response of DNT with the film, proposed to occur via π-π interactions reported previously between DNT and aromatic systems;[4] the latter consistent with the lower vapour pressure and hence pre-saturation concentration of available DNT quenchers compared to NB. In either case, the excellent response of ordered **BBDPP** thin films was rationalised based on their film structure and morphology, with the J-aggregate fibrous network facilitating improved optical transduction through a larger surface area of available and interacting electron rich π-π fluorophore sites as reported previously in other small molecule based systems.[22]

Ordered **HBDPP** thin films were characterised by inherently slower response to nitroaromatic vapours compared to amorphous equivalents. For DNT a high reduction in fluorescence was observed with 80 % of total emission quenched; the time required to achieve a 50 % reduction was longer than for the amorphous films (756 minutes versus 200 minutes). In this case, the surface area of interacting **HBDPP** molecules with accessibility to DNT was diminished by their enhanced structural periodicity compared to the amorphous films. For NB, quenching was again slower with ordered **HBDPP** films and the overall fluorescence quenched lower than for amorphous films with only 30 % reduction in emission after 70 minutes. Prolonged exposure to NB vapour also resulted in changes to the absorption and emission spectra of the films, indicative of structure and morphology changes, confirmed by SEM and XRD analysis and no further reduction in fluorescence intensity (Fig. 2c).

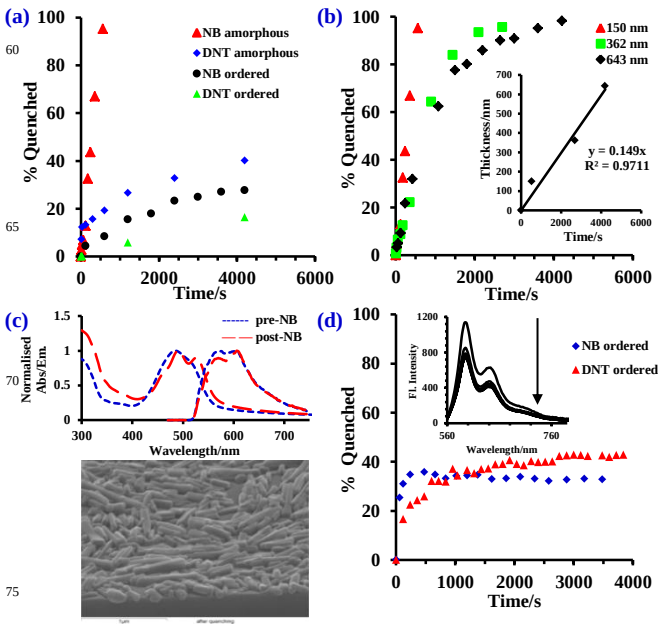

Fig. 2 a) Fluorescence quenching as a function of time for amorphous and ordered **HBDPP** films exposed to DNT and NB vapour b) effect of film thickness on rate of NB quenching for amorphous **HBDPP** films c) effect of NB exposure on absorption, emission and morphology of *as-deposited* ordered **HBDPP** films d) fluorescence quenching as a function of time for *as-deposited* ordered **BBDPP** films exposed to DNT and NB vapour

To probe effects of post deposition solvent annealing on structure, morphology and fluorescence quenching, and determine if the reduction in ordered **HBDPP** film emission upon exposure to NB was the result of structural changes, *as-deposited*, ordered **HBDPP** films were exposed to saturated headspace of acetone or toluene vapour. This resulted in formation of self-assembled microcrystals on the SiO_2 substrates similar to those observed after NB treatment (Fig. 3b). XRD analysis revealed reflections from 00*1*, 0*1*0 and 0*2*0 planes in films prepared on scattering SiO_2 treated with acetone or toluene (SI.6), whilst on non-scattering SiO_2 a preferred 00*l* progression was observed with reflections from 00*1*, 00*2*, 00*3*, 00*5* and 00*7* planes detected (Fig. 3a); both sets of XRD data confirmed via comparison with bulk powder and predicted PXRD patterns computed by Mercury[23] for the **HBDPP** single crystal (SI.6). For these **HBDPP** films, enhanced vibronic structure in the absorption spectra and emergence of a band at 463 nm, accompanied by an increase in the relative intensity of fluorescence at 606 nm is consistent with H-aggregate formation[19] (Fig. 3c). No drop in emission intensity was observed upon exposure to acetone or toluene, inferring that reduced emission from ordered **HBDPP** films exposed to NB was mainly due to fluorophore/quencher interactions and not structural changes. Accordingly, we propose that acetone and toluene annealed thin films of **HBDPP** are characterised by a structure consistent with the single crystal. Given that *h*00 planes from the crystal structure of **HBDPP** along the π-stacking *a*-axis are absent in the film XRDs further implies that the needle like crystals observed by SEM (Fig. 3b) are orientated with the π-stacking *a*-axis parallel to the substrate and directed along the long dimension in the crystal aspect (SI.6). Thus, **HBDPP** solvent annealed films could exhibit promising *optoelectronic* sensing properties, with efficient charge transport

in electronic devices observed from cofacial π-stacking along the current direction in the conducting channel.[24] Acetone and toluene treatment of ordered **BBDPP** films also enhanced their crystallinity, confirmed by XRD and SEM, with smaller changes observed in optical spectra (SI.6). Of note, was the dramatic change to **BBDPP** film morphology after annealing (Fig. 3b). In contrast to **HBDPP** however, diffraction data was not consistent between annealed **BBDPP** films, powder and single crystal; the optical spectra supporting a new crystal phase in the ordered **BBDPP** thin films with J-aggregate structure (SI.6).

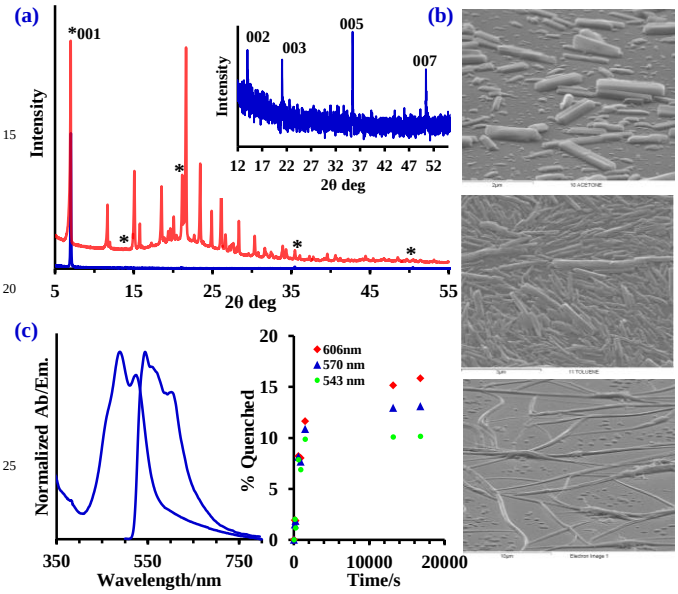

Fig. 3 a) PXRD pattern for **HBDPP** powder (red) and XRD pattern for acetone-annealed film (blue) with inset showing film 00*l* progression (common reflections indicated by *) b) SEM images of acetone (top) and toluene (middle) annealed films of **HBDPP** and acetone-annealed film of **BBDPP** (bottom) c) absorption and emission spectra of toluene-annealed **HBDPP** film (left) and fluorescence quenching as a function of time for a 150 nm toluene-annealed **HBDPP** film exposed to DNT vapour (right)

Fluorescence from 150 nm thick toluene annealed films of **HBDPP** exposed to DNT and NB vapour was quenched by 10-15 %, reaching saturation after 280 and 60 minutes respectively; the slow response similar to *as-deposited* ordered films and the overall reduction in total emission consistent with a decrease in film surface area and accessible quenchable sites. The surface area from a selection of crystallites determined by SEM analysis of acetone-annealed **HBDPP** films indicated that the proposed π-stacking end faces of the crystals contribute on average to 7-8 % of the total crystal surface area in the chosen population (SI.6). Given that the π-stacking interaction is the strongest in the **HBDPP** single crystal,[18] the comparable reduction in emission intensity in crystalline **HBDPP** films is therefore, mainly attributed to formation of a π-π stack between **HBDPP** and the nitroaromatic, also consistent with the larger reduction in intensity at saturation of H-aggregate emission at 606 nm compared to the bands at 570 nm and 543 nm (Fig. 3c). In toluene and acetone treated **BBDPP** films, DNT and NB quenching behaviour was also similar to that observed in the pre-annealed films with a rapid rise to emission saturation (SI.6). In crystalline films, the difference in emission quenching between DNT and NB (20 % *vs*. 10 % overall) is consistent with increased quencher reduction potential; the overall reduction in quenching compared to pre-annealed films attributed to reduced film surface area and accessibility of quenchable emissive sites (Fig. 3b).

In conclusion, we have identified for the first time, two DPP thin film platforms that can detect important nitroaromatics such as NB and DNT. Film crystal structure and morphology highly influence fluorescence quenching behaviour, such that by careful control of these properties effective signal transduction is realised. The rapid and efficient fluorescence quenching of DPP thin films qualifies their application as *optical* sensors in vapour sensing of nitroaromatics and confirms the potential of DPPs in the development of novel optoelectronic based sensing technologies, which we will report on in due course.

C.J.M. and M.W. acknowledge EPSRC for funding under the First Grant Scheme EP/J011746/1. The authors would like to thank the NCS at the University of Southampton for crystallographic data collection on **BBDPP**.

Notes and references

[a] *School of Science, University of the West of Scotland, Paisley, UK; Fax: 44 1418483204; Tel: 441418483210; E-mail: callum.mchugh@uws.ac.uk*
[b] *Pure and Applied Chemistry, University of Strathclyde, Glasgow, UK*
[c] *Photon Science Institute, University of Manchester, Manchester, UK*
[d] *School of Pharmacy, University of Reading, Reading, UK.*
[e] *Crystallografx Ltd., Milngavie, Glasgow, UK.*

† Electronic Supplementary Information (ESI) available: Full analysis of reported compounds and thin films. See DOI: 10.1039/b000000x/

1 J. Yinon, *Anal. Chem.*, 2003, 75, 99a.
2 J. Yinon, *Trends Anal. Chem.*, 2002, 21, 4, 292.
3 S. Singh, *J. Hazard. Mater.*, 2007**,** 144, 15.
4 M. E. Germain and M. J. Knapp, *Chem. Soc. Rev*., 2009, 38, 2543.
5 S. W. Thomas, G. D. Joly and T. M. Swager, *Chem. Rev*., 2007, 107, 1339.
6 J. Yang and T. M. Swager, *J. Am. Chem. Soc*., 1998, 120, 11864.
7 http://gs.flir.com/ (accessed October 2014)
8 S. J. Toal and W. C. Trogler, *J. Mater. Chem*,. 2006, 16, 2871.
9 K. J. Albert and D. R. Walt, *Anal. Chem*., 2000, 72, 1947.
10 S. Tao, G. Li and H. Zhu, *J. Mater. Chem*., 2006, 16, 4521.
11 Y. Engel, R. Elnathan, A. Pevzner, G, David, E. Flaxer and F. Patolsky, *Angew. Chem. Int. Ed*., 2010, 49, 6830.
12 Y. Che, X. Yang, G. Lui, H. Ji, J. Zuo, J. Zhao and L. Zang, *J. Am. Chem. Soc*., 2010, 132, 5743.
13 J. Li, C. E. Kenclig and E. E. Nesterov, *J. Am. Chem. Soc*., 2007, 129, 15911.
14 Y. H. Lee, H. Liu, J. Y. Lee, S. H. Kim, S. K, Kim, J. L. Sessler, Y. Kim and J. S. Kim, *Chem. Eur. J*., 2010, 16, 5895.
15 S. S. Nagarkar, A. V. Desai and S. K. Ghosh, *Chem. Commun*., 2014, 50, 8915.
16 J. C. Ho, A. Arango and V. Bulovic, *Appl. Phys. Lett.*, 2008, 93, 063305.
17 J. C. Ho, J. A. Rowehl and V. Bulovic, *Microsystems Technology Laboratories Annual Research Report*, 2009,
18 J. Calvo, M. Warzecha, A. R. Kennedy, C. J. McHugh and A. J. McLean, *Cryst. Growth. Des*, 2014, 14, 4849.
19 F. C. Spano, *Acc. Chem. Res.*, 2010, 43, 429.
20 M. Marshall and J. C. Oxley, *Aspects of Explosives Detection*, *Elsevier*, 2009.
21 S. Roy, A. K. Katiyar, S. P. Mondal, S. K. Ray and K. Biradha, *Appl. Mater. Interfaces*., 2014, 6, 11493
22 C. Vijayakumar, G. Tobin, W. Schmitt, M. J. Kim and M. Takeuchi, *Chem. Commun*., 2010, 46, 874.
23 C. F. Macrae, P. R. Edgington, P. McCabe, E. Pidcock, G. P. Shields, R. Taylor, M. Towler and J. van de Streek, *J. Appl. Cryst*., 2006, 39, 453.
24. C. Wang, D. Huanli, H. Wenping, L. Yunqi and Z. Daoben, *Chem. Rev*., 2012, 112, 2208.